Volt–Ampere and Thermal Characteristics of a Direct-Current Dual-Jet Plasma Generator

Hao Zhang, Gui-Qing Wu, He-Ping Li, *Member, IEEE*, and Cheng-Yu Bao

***Abstract*—With the thermal plasma hazardous medical waste treatment as the research background, the volt–ampere and thermal characteristics of a dual-jet direct-current (dc) thermal plasma generator are studied experimentally in this paper. Based on the experimental measurements concerning the arc voltages and thermal efficiencies of the plasma generator under different operating conditions, the generalized dimensional complex equations for the arc voltage and thermal efficiency as functions of the operating parameters are determined with the specified assumptions and by applying the multiple linear regression method to the measured data. The derived generalized functions for the volt–ampere and thermal features are helpful for the design and operation of the dual-jet dc arc thermal plasma generators in actual applications.**

***Index Terms*—Dual-jet plasma generator, similarity criteria, thermal efficiency, thermal plasma, volt–ampere characteristics.**

I. Introduction

DUE TO the unique features of high temperature or high energy density, abundant chemically reactive species, etc., thermal plasmas have been widely used in different industrial fields in the past few decades, such as plasma spraying, cutting, welding, surface modification, micro- or nanoscale materials synthesis, chemical vapor deposition, waste treatment, etc. [1], [2]. In recent years, thermal plasma hazardous medical waste (HMW) treatment technology has attracted much attention of the researchers in the world [3]–[10]. Due to the very complex compositions, including anatomical, pathological, infectious, radioactive, and other types of waste, such as knives, injectors, injector needles, plastics, fibers, etc., and particularly the heterogeneity and high danger nature of HMW, the requirements on the performances of the technologies for the treatment of HMW are very strict [4], [6]. Although the high-temperature incineration is a relatively inexpensive and mature technology, the secondary pollution emitted from the incinerators in the form of dioxins, furans, and heavy metals (e.g., Cd, Pb, Cr, etc.), as well as the infectious materials which may reside in the ash or slag, is unavoidable [5]. Compared to the conventional high-temperature incineration, the thermal plasma treatment of HMW provides intrinsic features, such as high process temperature and energy density, high throughputs with compact reactor geometry, high quench rates allowing specific gas compositions and solid materials to be obtained, rapid start-up and shutdown periods, no presorting of waste, no further consolidation of residues prior to proper landfill disposal, etc. [4], [7], [11]. Due to the benefits of saving costs in the handling and conditioning of the waste [7], and of the environmental protection, the thermal plasma HMW treatment technology would become a prospective treatment method of HMW for conforming to the ecological and sanitary standards established by the legislative bodies of the country. However, from the economic point of view, the application of thermal plasmas is a relative high-cost method due to its consumption of electric power and plasma-working gas. Therefore, in order to compete with other HMW treatment methods (e.g., the high-temperature incineration technology), the thermal plasma furnace should have high thermal efficiency, large volume of high-temperature region, abundant chemically reactive species, low erosion rate of electrodes, etc. [9].

In previous studies, the configurations of the thermal plasma torches used for HMW treatment could be single [1], [4]–[7] (or even multiple) traditional nontransferred direct-current (dc) arc plasma torch(es), dc arc plasma torches with hollow electrodes [9], [10], and dc arc dual-jet thermal plasma torches [8], [12]–[14]. Compared to the very limited high-temperature volume in the jet region generated by the single thermal plasma torch, different types of plasma torches were designed in order to enlarge the highly chemical reactive region of the thermal plasma jet, e.g., a combination of angled multiple independent nontransferred dc arc plasma torches [15], as shown in Fig. 1(a), and a plasma generator with one set of cathode and anode directed at an angle to one another [8], [12]–[14], as shown in Figs. 1(b) and (c), respectively. Theoretical and experimental studies showed that numerous operation parameters, such as the arc current (I), the distance (L), angle (β) between electrodes, the chemical composition of the plasma-forming gas and its flow rate (G) injected from the cathode and anode sides, etc., could influence the heat transfer and flow patterns inside the dc arc plasma furnace, the arc voltages between electrodes, and the thermal efficiencies of the plasma generators [8]–[10], [12], [13]. Due to the very complicated interactions among different operation parameters (e.g., I, L, β, G, etc.), it is essential to establish a generalized relationship between the preceding parameters and the major features of the plasma generator, such as the arc voltage $(V_{\rm arc})$ or the thermal efficiency (η).

Manuscript received September 25, 2008; revised November 26, 2008. Current version published July 9, 2009. This work was supported by the National Natural Science Foundation of China under Grants 10405015 and 10710293.

H. Zhang was with the Department of Engineering Physics, Tsinghua University, Beijing 100084, China. He is now with the Department of Electrical and Computer Engineering, University of Maryland, College Park, MD 20742 USA.

G.-Q. Wu, H.-P. Li, and C.-Y. Bao are with the Department of Engineering Physics, Tsinghua University, Beijing 100084, China (e-mail: liheping@tsinghua.edu.cn).

Color versions of one or more of the figures in this paper are available online at http://ieeexplore.ieee.org.

Digital Object Identifier 10.1109/TPS.2008.2011487

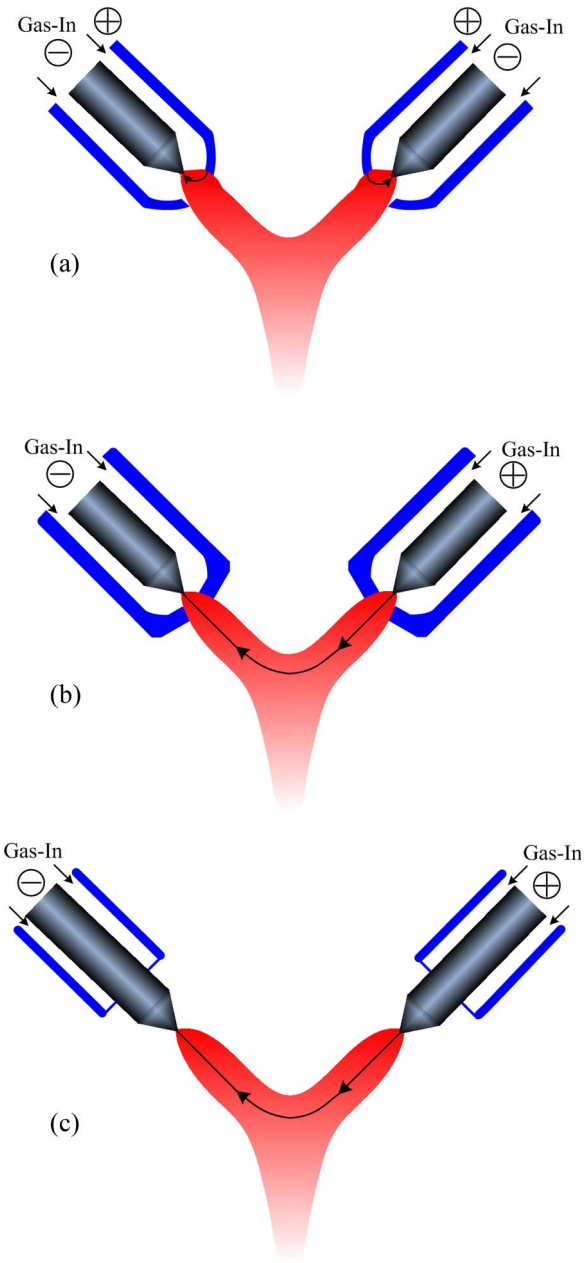

Fig. 1. Schematic diagrams of different dc arc thermal plasma generators. The black solid lines with arrows represent the current passage channel.

In previous studies, the generalizations of the volt–ampere and thermal characteristics for the plasma generators with hollow electrodes [9] and for the dual-jet plasma generators with the geometrical configuration [13] as shown in Fig. 1(b) were reported. For the dc arc thermal plasma generators with conical-shaped electrodes, as shown in Fig. 1(c), although some preliminary experimental [8] and numerical [16] results concerning the characteristics of the thermal plasma generators were published, the systematic investigations on the electrical and thermal characteristics are still seldom. In this paper, based on the experimental measurements of the arc voltages and thermal efficiencies of the dc arc thermal plasma generator with dual angled conical-shaped electrodes, as shown in Fig. 1(c), the generalized volt–ampere and thermal characteristics of the plasma generator are presented by using the similarity criteria, the validity of which is also tested with the measured data under different operating conditions.

II. Experimental Method

A. Experimental Setup

A schematic diagram of the experimental setup is shown in Fig. 2, which consists of the dc power supply system, the plasma-working-gas supply and control system, the dc arc dual-jet thermal plasma generator, the vacuum chamber, and the cooling-water cycle system. During the operation process, the plasma generator is located inside the vacuum chamber so that the gas discharges can operate in an argon atmosphere at 1.0 atm. The dual-jet plasma generator is composed of two electrodes with the same geometrical configuration, as shown in Fig. 3(a). The cerium–tungsten (1.8%–2.2% of CeO_2) 7.0-mm-in-diameter 60°-conical-shaped electrode is supported by the water-cooled copper double-layer cylinder. The plasma-working gas (argon with purity of 99.99% or better) is admitted axially from the cathode and anode sides through the circular space outside of the water-cooled copper cylinder. The images of the arc plasmas are taken by a digital camera (Fujifilm S5500). If the treated materials (e.g., the radwaste, HMW, etc.) are placed in the plasma jet region, they can be decomposed quickly and completely due to the very high energy density of the high-temperature partially ionized gas [1]. In this paper, by measuring the voltages between the electrodes and the ballast resistance using the voltage probe (Tek P6139A) and the digital oscilloscope (Tektronix DPO4034), as shown in Fig. 2, the total arc voltage between electrodes $(V_{\rm arc})$, which includes the voltage drops both in the arc column region and the electrode sheath regions, and the arc current (I) can be obtained, and correspondingly, the total power input can be expressed as $P_{\rm in} = V_{\rm arc} \cdot I$. The temperature difference of the cooling water between the inlet and outlet of the plasma torch (ΔT) is measured by a homemade K-type thermocouple. Thus, the thermal efficiency (η) of the plasma generator can be calculated by $\eta = 1 - (G_0 \cdot C_0)/(V_{\rm arc} \cdot I) \cdot \Delta T$, where G_0 and C_0 $[= 4.2 \times 10^3\ {\rm J}/({\rm kg} \cdot {}^\circ{\rm C})$ for water] are the mass flow rate and the specific heat of water, respectively.

B. Generalization Method for the Volt–Ampere and Thermal Characteristics

As indicated in Section I, there are numerous factors (e.g., I, L, β, G, etc.) that would influence the characteristics of the thermal plasma generator. For promoting actual applications, it will be a very difficult and expensive task if the design and test of the plasma generators depend on the experimental studies only. Thus, generalization of the volt–ampere and thermal characteristics of the plasma generator has been adopted in previous papers based on the method of the dimensionless criteria or the dimensional complexes [9], [13], since it allows one to perform an engineering calculation of the plasma generator.

Based on the dimensionless equations describing the physical phenomena occurring in a thermal plasma generator, the following nondimensional numbers need to be taken into account [9], [13], [17], [18] with the consideration of the variations of

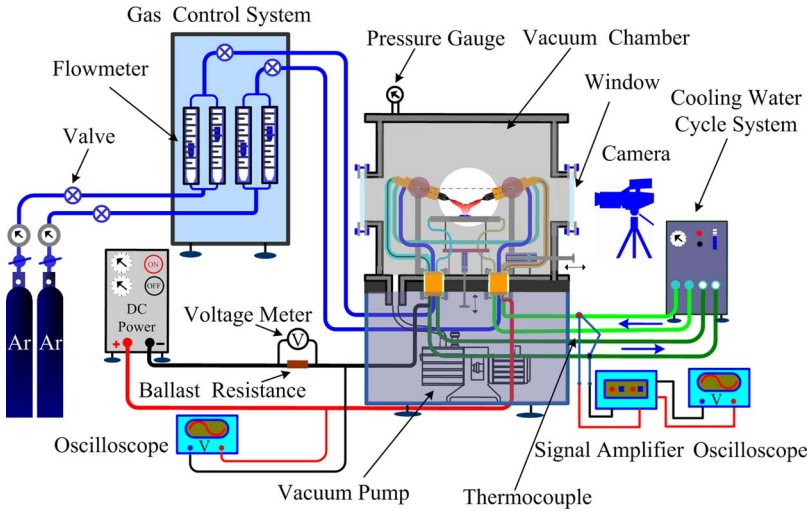

Fig. 2. Schematic diagram of the experimental setup.

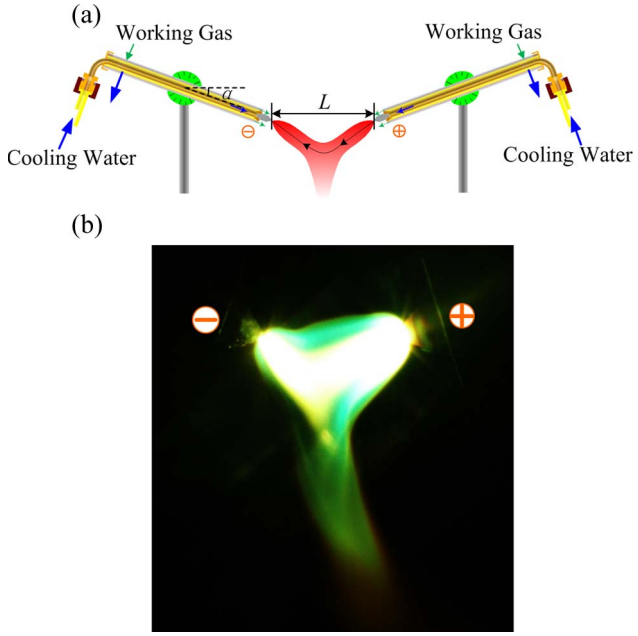

Fig. 3. (a) Schematic diagram of the dual-jet dc arc thermal plasma generator and (b) the typical discharge image for the case of $I = 56$ A, $G = 10.0$ slpm, $\alpha = 20^\circ$, and $L = 2.0$ cm.

the declination angles between electrodes in the dual-jet dc arc thermal plasma generator:

$$\Pi_h = \frac{\sigma_0 h_0 G d}{I^2} \tag{1}$$

$$\Pi_{\mathrm{Re}} = \frac{G}{\mu_0 d} \tag{2}$$

$$\Pi_L = \frac{L}{d\cos\alpha} \tag{3}$$

$$\Pi_{\mathrm{U}} = \frac{\sigma_0 V_{\mathrm{arc}} d}{I} \tag{4}$$

$$\Pi_\eta = \frac{1-\eta}{\eta} \tag{5}$$

where σ, μ, and h are the electrical conductivity, viscosity, and specific enthalpy of plasmas, respectively, G is the flow rate of the plasma-working gas, d is the diameter of the electrodes, L is the horizontal standoff distance between electrodes, α is the angle between the electrode axis and the horizontal line [as shown in Fig. 3(a)], I is the arc current, V_{arc} is the arc voltage between electrodes, and η is the thermal efficiency of the plasma generator. The subscript "0" represents the corresponding values at a reference gas temperature [17], [18]. Based on the preceding nondimensional numbers, the generalized functions of the arc voltage (V_{arc}) or the thermal efficiency (η) with the variations of the operation parameters, including the arc current (I), the horizontal standoff distance (L) between electrodes, the angle (α) between the electrode axis and the horizontal line, and the flow rate (G), can be expressed as the following forms:

$$\frac{\sigma_0 V_{\mathrm{arc}} d}{I} = C\left(\frac{I^2}{\sigma_0 h_0 G d}\right)^{a_1}\left(\frac{G}{\mu_0 d}\right)^{a_2}\left(\frac{L}{d\cos\alpha}\right)^{a_3} \tag{6}$$

$$\frac{1-\eta}{\eta} = C'\left(\frac{I^2}{\sigma_0 h_0 G d}\right)^{a'_1}\left(\frac{G}{\mu_0 d}\right)^{a'_2}\left(\frac{L}{d\cos\alpha}\right)^{a'_3}. \tag{7}$$

In this section, for establishing the relationship between V_{arc} or η and the operation parameters (I, L, α, and G), the following are assumed: 1) Argon is used as the plasma-working gas and the surrounding gas; 2) the flow rates of argon on the cathode and anode sides are the same; 3) the angles between the electrode axis and the horizontal line for the anode and cathode are the same; 4) the pressure in the chamber is kept constant (1 atm) during operation; 5) the diameters of the electrodes are also constant during operation; and 6) the anode and cathode jets are quasi-symmetric. Based on the preceding assumptions, the generalized functions [(6) and (7)] can be rewritten as the following dimensional complexes:

$$V_{\mathrm{arc}} = B \cdot I^m \cdot G^n \cdot \left(\frac{L}{\cos\alpha}\right)^q \tag{8}$$

$$\frac{1-\eta}{\eta} = B' \cdot I^{m'} \cdot G^{n'} \cdot \left(\frac{L}{\cos\alpha}\right)^{q'} \tag{9}$$

where B, B' and m, m', n, n', q, q' are the coefficients and exponents of the dimensional complexes, respectively, which depend on the geometrical configuration of the plasma generator, the chemical compositions of the plasma-working gas, etc.

In this paper, for determining the values of B, B', m, m', n, n', q, and q', the parameters of I, L, α, and G vary in the following ranges: $I = 38 - 56$ A, $L = 1.0 - 4.4$ cm, $\alpha = 10 - 30°$, and $G = 5.0 - 15.0$ slpm. Thus, the coefficients and exponents appearing in (8) and (9) B, B' and m, m', n, n', q, q' are determined by applying a multiple linear regression method [19] to the measured values of the arc voltages and thermal efficiencies.

III. Experimental Results and Discussions

A. Discharge Images

A typical image of the arc plasmas produced by the dual-jet plasma generator for the case of $I = 56$ A, $G = 10.0$ slpm, $\alpha = 20°$, and $L = 2.0$ cm is shown in Fig. 3(b). It can be seen from Fig. 3 that, after gas breakdown, a current passage channel between the electrodes forms. The cold gas admitted from the circular space on the anode and cathode sides is heated quickly due to the Joule heating effect and accelerated, forming the cathode and anode jets. The two jets encounter at the downstream of the electrode tips, merging into a high-temperature plasma jet and flowing downward. Fig. 3(b) shows that the discharge image of the arc plasma is not exactly symmetric, although the geometry and the gas inlet conditions of the plasma torch are symmetric. One of the possible reasons which lead to this asymmetric feature of the arc plasmas may be the different physical processes in the torch cathode and anode regions. For this interesting phenomenon, further studies will be conducted in the future work. The experimental observations show that, with other parameters being unchanged, the volume of the high-temperature region of the plasma jet enlarges with the increase of the horizontal standoff distance of the electrodes, and the luminosity of the plasma jet region increases with increasing the arc current.

B. Volt–Ampere Characteristics

Due to the fluctuations of the arc voltages, the arc voltage is an averaged value of 32 measured values with a sampling time of 1 ms for each measured datum by an oscilloscope (Tektronix DPO4034). The variation of the arc voltages $(V_{\rm arc})$ as a function of the horizontal standoff distance of electrodes (L) for the case of $G = 8.0$ slpm, $\alpha = 20°$, and $I = 50$ A is shown in Fig. 4. With other parameters being unchanged, resulting from the increase of the current passage length $L'(= L/\cos\alpha)$, the arc voltage increases with the increase in L. The same variation tendency is also observed at different arc currents, as shown in Figs. 5(a) and (b), due to the increase of L or α (or the decrease of cosα). The experimental measurements in this paper also show that, although the influences of the arc currents on the arc voltages are not obvious (less than 2.0 V in the parameter ranges shown in Fig. 5) with other parameters being unchanged, an appropriate combination of the arc current,

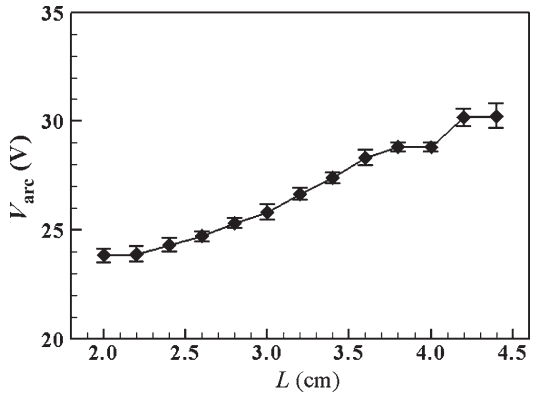

Fig. 4. Variation of the arc voltage with the horizontal standoff distance between electrodes ($G = 8.0$ slpm, $\alpha = 20°$, and $I = 50$ A).

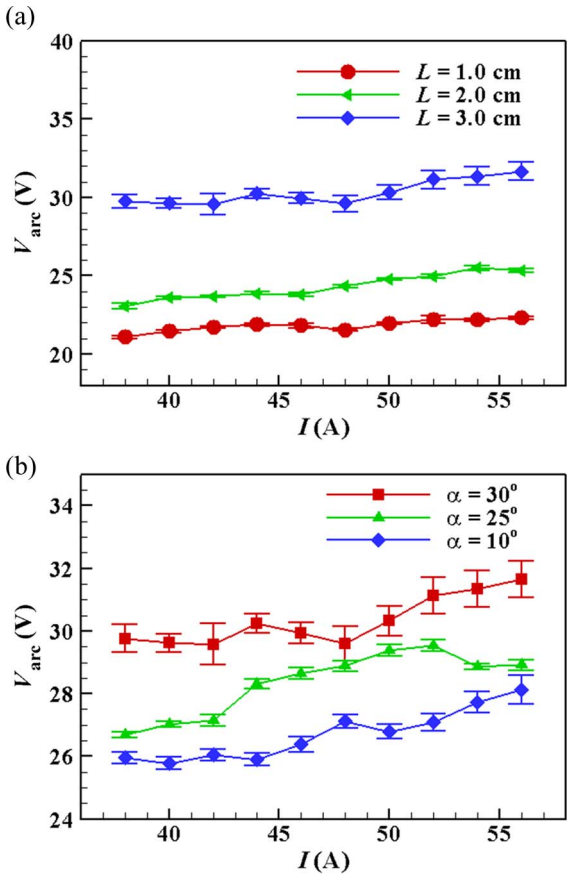

Fig. 5. Volt–ampere characteristics of the dual-jet dc arc thermal plasma generator for (a) different horizontal standoff distances between electrodes with $G = 8.0$ slpm and $\alpha = 30°$ and (b) different declination angles between electrodes with $G = 8.0$ slpm and $L = 3.0$ cm.

plasma-working-gas flow rate, the horizontal standoff distance, and declination angle between electrodes $(\beta = 180° - 2\alpha)$ is very important for obtaining a quasi-steady discharge mode. The stability of the arc will influence the measured values of the arc voltages, as well as the thermal efficiencies to be discussed in the next section.

In this section, based on the experimental data obtained under different operation conditions in the parameter ranges $I = 38 - 56$ A, $L = 1.0 - 4.4$ cm, $G = 5.0 - 15.0$ slpm, and

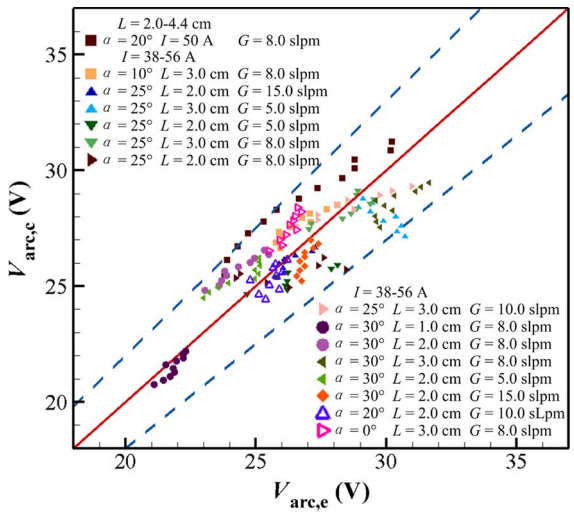

Fig. 6. Comparison of the measured and predicted arc voltages of the dual-jet dc arc plasma generator. The solid line represents the cases with equal predicted and measured values of the arc voltages, while the two dashed lines indicate the upper and lower boundaries of the calculated values deviating from the measured data (±10%).

$\alpha = 10 - 30°$, the dimensional complex equation for the arc voltage can be expressed as

$$V_{\rm arc} = 10.02 \cdot I^{0.175} \cdot G^{0.026} \cdot \left(\frac{L}{\cos\alpha}\right)^{0.258} \qquad (10)$$

where the units of $V_{\rm arc}$, I, G, L, and α are volts, amperes, standard liters per minute, centimeters, and degrees, respectively. It is seen from (10) that the arc voltage depends more on the length of the arc current passage channel (i.e., L and α), while less on the arc current and the plasma-working-gas flow rate. The calculated values of the arc voltages $(V_{\rm arc,c})$ from (10) and the measured data $(V_{\rm arc,e})$ used for obtaining the dimensional complex equation under the same operation conditions are shown in Fig. 6, where the vertical and horizontal axes represent the calculated and measured arc voltages, the solid line represents the cases with equal calculated and measured values of the arc voltages, and the two dashed lines indicate the upper and lower boundaries of the calculated values deviating from the experimental data (±10%). It can be seen from Fig. 6 that the predicted arc voltages by employing (10) are reasonably consistent with the measured data.

C. Thermal Efficiency

According to the definition of the thermal efficiency of the plasma generator in Section II-A, the mass flow rate of the cooling water needs to be measured during operation. In this paper, with a specified pressure at the outlet of the cooling-water chamber, the value of G_0 is always constant (0.025 kg/s in this study). The influences of the arc currents and the argon flow rates on the thermal efficiencies of the dc arc plasma generator with the constant values of $L = 2.0$ cm and $\alpha = 25°$ are shown in Fig. 7(a). It is shown in Fig. 7(a) that, for a certain constant arc current, the thermal efficiency increases with the increase of the argon flow rate. This is because, although the influence of the argon flow rate on the arc voltage is small, as indicated

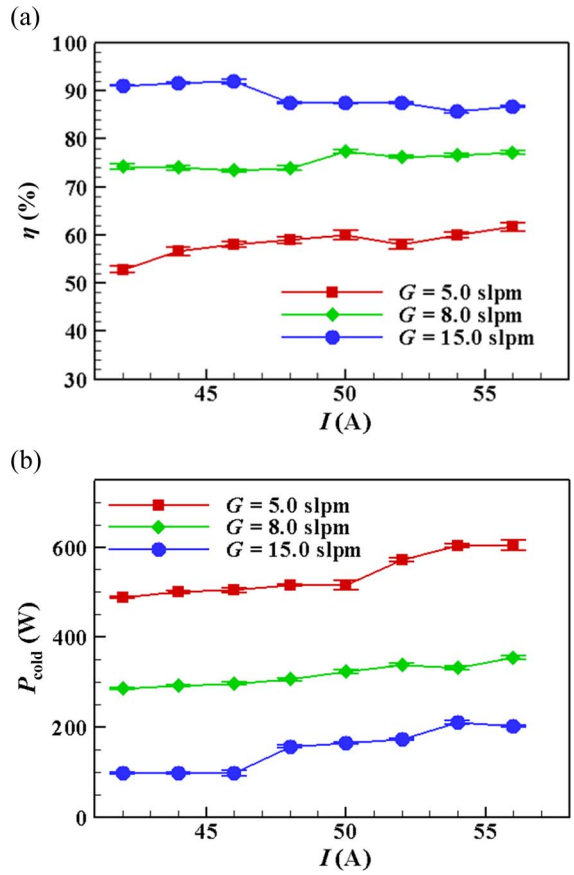

Fig. 7. Variations of the (a) thermal efficiency and (b) heat loss as functions of the arc currents at different argon flow rates with $L = 2.0$ cm and $\alpha = 25°$.

in (10), the heat loss taken away by the cooling water $(P_{\rm cold})$ decreases significantly with increasing the argon flow rate, as shown in Fig. 7(b), which results in an obvious increase of the thermal efficiency.

With the similar method as that provided in the foregoing section, the dimensional complex equation for the thermal efficiency of the plasma generator based on the measured data using the multiple linear regression method is expressed as

$$\frac{1-\eta}{\eta} = 7.081 \cdot I^{0.289} \cdot G^{-1.616} \cdot \left(\frac{L}{\cos\alpha}\right)^{-0.868}. \qquad (11)$$

Equation (11) indicates that the thermal efficiency of the thermal plasma generator depends more on the argon flow rate, while less on the length of the current passage channel and the arc current. The calculated values of the thermal efficiencies $(\eta_{\rm c})$ from (11) and the measured ones $(\eta_{\rm e})$ under the same operating conditions are shown in Fig. 8, where the two dashed lines indicate the upper and lower boundaries of the calculated values deviating from the experimental data (±15%). Fig. 8 shows that the thermal efficiency of the plasma generator is in the range of 50%–90% for the cases studied in this paper, and the predicted thermal efficiencies using (11) are also reasonably consistent with the measured data.

In order to make the generalized dimensional complex equations for the volt–ampere and thermal characteristics of the dc arc plasma generator [(10) and (11)] be useful for the analysis

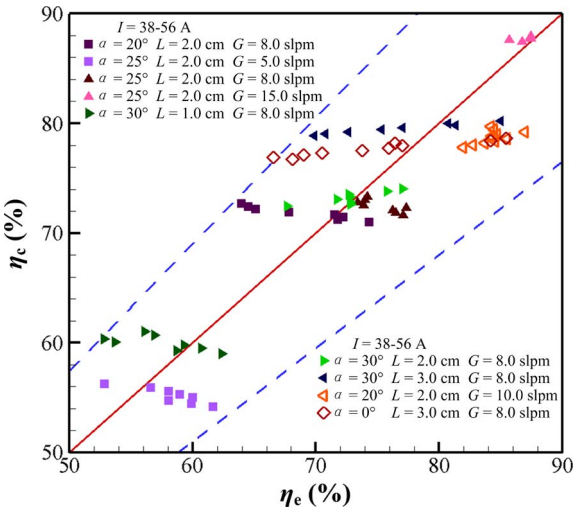

Fig. 8. Comparison of the measured and predicted thermal efficiencies of the dual-jet dc arc plasma generator. The solid line represents the cases with equal predicted and measured values of the thermal efficiencies, while the two dashed lines indicate the upper and lower boundaries of the calculated values deviating from the measured data (±15%).

of the operating parameters of the dual-jet plasma generator, as shown in Fig. 1(c), it is necessary to test the validity of the preceding generalized functions under other operating conditions. For the cases of $I = 38 - 56$ A, $L = 2.0$ cm, $G = 10.0$ slpm, $\alpha = 20^\circ$ and $I = 38 - 56$ A, $L = 3.0$ cm, $G = 8.0$ slpm, $\alpha = 0^\circ$, which are different from the cases in Sections III-B and III-C for calculating the coefficients and exponents of the dimensional complex equations, the calculated values of $V_{\rm arc}$ and η by using (10) and (11), as well as the measured data under the same operating conditions, are also shown in Figs. 6 and 8, respectively, represented by the open symbols. From Figs. 6 and 8, it can be concluded that, for the dual-jet dc arc thermal plasma generator as shown in Fig. 1(c), the generalized functions for the arc voltage and thermal efficiency can reasonably predict the volt–ampere and thermal characteristics of the plasma generator if pure argon is employed as the plasma-working gas and the surrounding gas.

IV. Concluding Remarks

In this paper, experimental studies concerning the influences of the arc current (I), the horizontal standoff distance (L) and declination angle $(\beta = 180^\circ - 2\alpha)$ between electrodes, and the flow rate (G) of the plasma-working gas on the arc voltage $(V_{\rm arc})$ and thermal efficiency (η) of the dual-jet dc arc thermal plasma generator are conducted. The generalized dimensional complex equations for $V_{\rm arc}$ and η as functions of the operating parameters (I, L, G, and α) are determined by applying the multiple linear regression method to the measured data and are also validated by the extra experimental measurements for the cases with $L = 1.0 - 4.4$ cm, $I = 38 - 56$ A, $Q = 5.0 - 15.0$ slpm, and $\beta = 120^\circ - 180^\circ$ and also with argon as the plasma-working gas and the surrounding gas. The main conclusions are as follows:

1) Among different operating parameters (e.g., I, L, G, and α), the arc voltage depends more on the length of the current passage channel (i.e., L and α), while the thermal efficiency of the plasma generator is mainly affected by the plasma-working-gas flow rate (G).
2) The maximum deviations of the predicted values of the arc voltages and thermal efficiencies of the plasma generator by using the dimensional complex equations are less than 10% and 15%, respectively. This implies that the generalized functions for the volt–ampere and thermal characteristics of the dual-jet dc arc thermal plasma generator are useful for the analysis of the characteristics of the plasma generator, as shown in Fig. 3 in the parameter ranges studied in this paper, and are also helpful for the design and operation of such type of plasma generators in actual applications.

In this paper, the generalized dimensional complex equations for the arc voltage and thermal efficiency of the dual-jet dc arc plasma generator are obtained based on the limited variations of the operation parameters and also with some assumptions for simplifying the analysis. In further studies, more investigations on the asymmetric feature of the arc plasmas, the influences of the complex configurations (e.g., different declination angles and/or different plasma-working-gas flow rates on the cathode and anode sides, etc.), and the chemical compositions of the plasma-working gas and/or surrounding gas on the electrical and thermal characteristics of the plasma generators and the three-dimensional, transient, and nonequilibrium features, as well as the complicated interaction processes between the high-temperature partially ionized gas and the treated materials, etc., will be conducted.

Acknowledgment

The authors would like to thank Prof. X. Chen, Department of Engineering Mechanics, Tsinghua University of China, for the valuable suggestions.

References

[1] M. I. Boulos, P. Fauchais, and E. Pfender, *Thermal Plasmas*, vol. 1. New York: Plenum, 1994.
[2] X. Chen, *Heat Transfer and Fluid Flow Under Thermal Plasma Conditions*. Beijing, China: Sci. Press, 1993. (in Chinese).
[3] E. Pfender, "Thermal plasma technology: Where do we stand and where are we going?" *Plasma Chem. Plasma Process.*, vol. 19, no. 1, pp. 1–31, Mar. 1999.
[4] J. P. Chu, I. J. Hwang, C. C. Tzeng, Y. Y. Kuo, and Y. J. Yu, "Characterization of vitrified slag from mixed medical waste surrogates treated by a thermal plasma system," *J. Hazard. Mater.*, vol. 58, no. 1, pp. 179–194, Feb. 1998.
[5] A. B. Murphy and T. McAllister, "Modeling of the physics and chemistry of thermal plasma waste destruction," *Phys. Plasmas*, vol. 8, no. 5, pp. 2565–2571, May 2001.
[6] P. G. Rutberg, A. N. Bratsev, A. A. Safronov, A. V. Surov, and V. V. Schegolev, "The technology and execution of plasmachemical disinfection of hazardous medical waste," *IEEE Trans. Plasma Sci.*, vol. 30, no. 4, pp. 1445–1448, Aug. 2002.
[7] J. Fiedler, E. Lietz, D. Bendix, and D. Hebecker, "Experimental and numerical investigations of a plasma reactor for the thermal destruction of medical waste using a model substance," *J. Phys. D: Appl. Phys.*, vol. 37, no. 7, pp. 1031–1040, Apr. 2004.
[8] T. Inaba, M. Kikuchi, H. Li, and T. Iwao, "Twin torch plasma arc furnace for medical waste treatment," in *Proc. 16th Int. Conf. Gas Discharges Their Appl.*, Xi'an, China, 2006, vol. 1, pp. 461–464.

[9] M. Hur, K. S. Kim, and S. H. Hong, "Operational features and air plasma characteristics of a thermal plasma torch with hollow electrodes," *Plasma Sources Sci. Technol.*, vol. 12, no. 2, pp. 255–264, May 2003.
[10] K. S. Kim, J. M. Park, S. Choi, J. Kim, and S. H. Hong, "Enthalpy probe measurements and three-dimensional modelling on air plasma jets generated by a non-transferred plasma torch with hollow electrodes," *J. Phys. D: Appl. Phys.*, vol. 41, no. 6, p. 065 201, Mar. 2008.
[11] U. Kogelschatz, "Atmospheric-pressure plasma technology," *Plasma Phys. Control. Fusion*, vol. 46, no. 12B, pp. B63–B75, Dec. 2004.
[12] H. You, W.-Z. Yan, and C.-K. Wu, "Numerical investigation of flow field of a dual-jet plasma generator," *Plasma Sci. Technol.*, vol. 2, no. 1, pp. 141–149, Feb. 2000.
[13] S. P. Polyakov and M. G. Rozenberg, "Study and generalization of volt–ampere and thermal characteristics of a two-jet plasmotron," *J. Eng. Phys.*, vol. 32, no. 6, pp. 675–682, Jun. 1977. (Translated from Inzhenerno-Fizicheskii Zhurnal, vol. 32, no. 6, pp. 1043–1052, 1977).
[14] S. P. Polyakov and V. I. Pechenkin, "Electrical and thermal structure of the argon arc of a two-jet plasmatron," *J. Eng. Phys.*, vol. 43, no. 5, pp. 1293–1296, Nov. 1982. (Translated from Inzhenerno-Fizicheskii Zhurnal, vol. 43, no. 5, pp. 833–837, 1982).
[15] N. J. Wagner, W. W. Gerberich, and J. V. R. Heberlein, "Thermal plasma chemical vapor deposition of wear-resistant, hard Si–C–N coatings," *Surf. Coat. Technol.*, vol. 201, no. 7, pp. 4168–4173, Dec. 2006.
[16] G.-Q. Wu, H.-P. Li, C.-Y. Bao, X. Chen, T. Iwao, M. Yumoto, and T. Inaba, "Two-dimensional modelling of a DC arc plasma furnace with opposite cathode and anode," *Prog. Comput. Fluid Dyn.*, vol. 8, no. 7/8, pp. 424–431, Nov. 2008.
[17] O. I. Yas'ko, "Correlation of the characteristics of electric arcs," *J. Phys. D: Appl. Phys.*, vol. 2, no. 5, pp. 733–751, May 1969.
[18] G. Li, W. Pan, X. Meng, and C. Wu, "Application of similarity theory to the characterization of non-transferred laminar plasma jet generation," *Plasma Sources Sci. Technol.*, vol. 14, no. 2, pp. 219–225, May 2005.
[19] D. G. Kleinbaum, L. L. Kupper, K. E. Muller, and A. Nizam, *Applied Regression Analysis and Other Multivariable Methods*. Beijing, China: China Mach. Press, 2003.

Hao Zhang received the B.S. degree from Tsinghua University, Beijing, China, in 2008. He is currently working toward the Ph.D. degree in the Department of Electrical and Computer Engineering, University of Maryland, College Park.

His research interests include experimental studies on the characteristics and applications of atmospheric pressure direct-current thermal plasmas.

Gui-Qing Wu received the B.S. degree from the Artillery Academy of China, Hefei, China, in 1997 and the M.S. degree from the Department of Engineering Physics, Tsinghua University, Beijing, China, in 2008, where he is currently working toward the Ph.D. degree.

His current research interests are the numerical and experimental studies on the fluid flow and heat/mass transfer under thermal plasma conditions.

He-Ping Li (M'07) received the B.S. degree from Xi'an Jiaotong University, Xi'an, China, in 1996 and the M.S. and Ph.D. degrees from Tsinghua University, Beijing, China, in 1998 and 2001, respectively.

He is an Associate Professor with the Department of Engineering Physics, Tsinghua University. His current research interests are the experimental and theoretical studies on heat transfer, fluid flow, and nonequilibrium effects in atmospheric-pressure gas discharge plasma systems.

Dr. Li is a member of the Institute of Electrical and Electronics Engineers of the U.S.

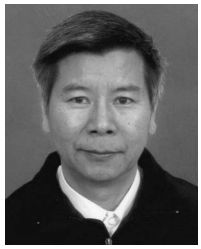

Cheng-Yu Bao received the diploma from the Department of Precision Instruments and Mechanology, Tsinghua University, Beijing, China, in 1970 and the M.S. degree from the Department of Physics, Tsinghua University, in 1982.

He is a Professor with the Department of Engineering Physics, Tsinghua University. His current research interests are laser isotropic separation and atmospheric pressure gas discharge plasmas.